

Extensibility and Distensibility of the Thoracic Aorta in Patients with Aneurysm

H.W.L. de Beaufort^{a,b,f}, F.J.H. Nauta^{a,b,c,f}, M. Conti^d, E. Cellitti^e, C. Trentin^e, E. Faggiano^d, G.H.W. van Bogerijen^{a,b}, C.A. Figueroa^c, F.L. Moll^b, J.A. van Herwaarden^b, F. Auricchio^{d,e}, S. Trimarchi^{a,*}

^aThoracic Aortic Research Center, Policlinico San Donato IRCCS, University of Milan, Italy

^bDepartment of Vascular Surgery, University Medical Center Utrecht, The Netherlands

^cDepartments of Biomedical Engineering and Surgery, University of Michigan, Ann Arbor, USA

^dDepartment of Civil Engineering and Architecture, University of Pavia, Italy

^eCESNA Center for Advanced Numerical Simulations, Istituto Universitario di Studi Superiori di Pavia (IUSS), Pavia, Italy

WHAT THIS PAPER ADDS

In this paper, radial and longitudinal pulsatile aortic deformations were quantified and a new definition of longitudinal deformation is proposed. This definition is based on the physiological principle that the changes in aortic length are caused by heart movement pulling the proximal end of the aorta up and down combined with the load of the blood flow ejected into the aorta. In a cohort of 10 patients with abdominal or thoracic aortic aneurysm, pulsatile aortic deformations are considerable in both directions, with important variations between individuals, and the largest deformations occurring in the ascending aorta.

Objectives: Reference values of aortic deformation during the cardiac cycle can be valuable for the pre-operative planning of thoracic endovascular aortic repair (TEVAR) and for facilitating computational fluid dynamics. This study aimed to quantify normal aortic extensibility (longitudinal extension) and distensibility (radial expansion), as well as pulsatile strain, in a group of 10 (>60 years) individuals with abdominal or thoracic aortic aneurysms.

Methods: ECG gated CT images of the thoracic aorta were reconstructed into virtual 3D models of aortic geometry. The centre lumen line length of the thoracic aorta and three longitudinal segments, and the aortic diameter and luminal areas of four radial intersections were extracted with a dedicated software script to calculate extensibility, longitudinal strain, distensibility, and circumferential area strain.

Results: Mean extensibility and longitudinal strain of the entire thoracic aorta were $3.5 [1.3–6.8] \times 10^{-3} \text{ N}^{-1}$, and $2.7 [1.0–4.5]\%$, respectively. Extensibility and longitudinal strain were most pronounced in the ascending aorta ($20.6 [5.7–36.2] \times 10^{-3} \text{ N}^{-1}$ and $15.9 [6.6–31.9]\%$) and smallest in the descending aorta ($4.4 [1.6–12.3] \times 10^{-3} \text{ N}^{-1}$ and $2.2 [0.7–4.7]\%$). Mean distensibility and circumferential area strain were most pronounced at the sinotubular junction ($1.7 [0.5–2.9] \times 10^{-3} \text{ mmHg}^{-1}$ and $11.3 [3.3–18.5]\%$, respectively). Distensibility varied between $0.9 [0.3–2.5] \times 10^{-3} \text{ mmHg}^{-1}$ and $1.2 [0.3–3.3] \times 10^{-3} \text{ mmHg}^{-1}$ at the intersections in the aortic arch and descending aorta.

Conclusions: Pulsatile deformations in both longitudinal and circumferential directions are considerable throughout the thoracic aorta. These findings may have implications for pre-operative TEVAR planning and highlight the need for devices that can mimic the significant aortic longitudinal and circumferential strains.

© 2016 European Society for Vascular Surgery. Published by Elsevier Ltd. All rights reserved.

Article history: Received 12 June 2016, Accepted 15 November 2016, Available online XXX

Keywords: Pulsatile flow, Thoracic aorta, Abdominal aneurysm, Thoracic aneurysm, Distensibility, Extensibility

INTRODUCTION

Clinical success of thoracic endovascular aortic repair (TEVAR) depends partly on correct sizing of the stent graft.

Mis-sizing may lead to stent graft related complications such as type I endoleaks, retrograde or antegrade dissection, stent graft migration, or collapse.^{1–4} Dynamic imaging is important to correctly assess the conformational changes of the aorta over the cardiac cycle. ECG gated computed tomography (CT) and magnetic resonance imaging (MRI) have been widely used in various aortic pathologies,^{5–8} with good accuracy because of high resolution and tissue contrast. Using these imaging modalities, the quantification of aortic distensibility assesses aortic stiffness as it takes the load (i.e. pulse pressure) into account, on which

^f H.W.L. de Beaufort and F.J.H. Nauta contributed equally to this study.

* Corresponding author. Thoracic Aortic Research Center, Policlinico San Donato IRCCS, Piazza Malan 2, 20097 San Donato Milanese, Italy.

E-mail addresses: santi.trimarchi@grupposandonato.it; santi.trimarchi@unimi.it (S. Trimarchi).

1078-5884/© 2016 European Society for Vascular Surgery. Published by Elsevier Ltd. All rights reserved.

<http://dx.doi.org/10.1016/j.ejvs.2016.11.018>

deformations greatly depend.⁹ This is important as aortic stiffening is a known predictor of cardiovascular disease and death.^{10–14} Moreover, quantification of aortic distensibility has been reported to have important value in pre-operative planning.¹⁵ Local aortic wall stress can also be derived from estimates of aortic stiffness and measured aortic strain.¹⁶ Most studies thus far have been limited, however, to examining the circumferential strain and radial distensibility, but have neglected the significant longitudinal strain experienced by the aorta over the cardiac cycle.¹¹

This study presents a computer aided, semi-automatic measurement method to measure aortic dimensions during the cardiac cycle, based on ECG gated CT imaging of non-dilated and aneurysmal thoracic aortas of eight patients with abdominal aortic aneurysm and two patients with descending thoracic aortic aneurysms (seven male, three female) unaffected by connective tissue disorder. Thus, the study aimed to quantify thoracic aortic distensibility (radial expansion) and circumferential strain as well as extensibility (longitudinal extension) and longitudinal strain.

MATERIALS AND METHODS

Study population and image acquisition

Images were retrospectively selected from a group of abdominal and thoracic aortic aneurysm patients (aged 66–89 years) who underwent routine imaging of the entire aorta at the University Medical Centre Utrecht, the Netherlands, with ECG gated CTA. Exclusion criteria were connective tissue disorder, or prior aortic surgery. Brachial

blood pressures at the time of imaging were collected. The study protocol was evaluated by the local ethical review board and formal approval and informed consent was waived.

Imaging was performed using a 64 row multislice CT scanner (Philip Medical Systems, Best, The Netherlands) with a standardised acquisition protocol (slice thickness 0.9 mm, increment 0.7 mm) using 90–150 mL of intravenous non-ionic contrast (Iopromide, Schering, Berlin, Germany) injected at 6 mL/s, followed by a 60 mL saline chaser bolus. Scanning started using bolus triggering software with a threshold of 100 HU over baseline. Eight equally spaced phases were acquired over the cardiac cycle for each patient.

Image processing and 3D geometric analysis

Eight three dimensional segmentations of the aortic luminal boundary were created for each patient using the dynamic CT data and ITK-Snap software.¹⁷ Next, the Vascular Modeling Toolkit libraries^{18,19} were used to extract aortic centre lines for each phase. After manual designation of the proximal and distal ends of the aortic segmentation, the libraries automatically create a centre lumen line from sinotubular junction to coeliac bifurcation.

Each centre lumen line was divided into three different regions (ascending aorta, aortic arch, and descending aorta, Fig. 1A). Reference cross sections perpendicular to the centre lumen lines were defined at anatomical landmarks at the sinotubular junction, brachiocephalic trunk, left subclavian artery, and coeliac artery (Fig. 1B).

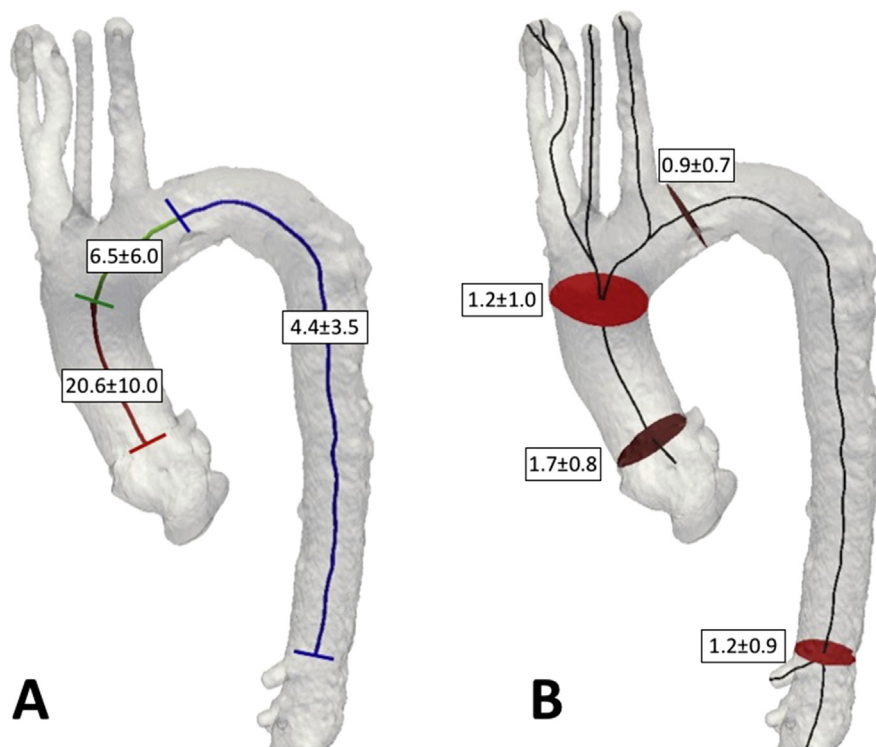


Figure 1. Longitudinal segments and radial intersections of the thoracic aorta delineated by anatomical landmarks, the sinotubular junction and centreline bifurcations of the brachiocephalic trunk, left subclavian artery, and coeliac trunk. Also included are the average values of regional extensibility (A) and distensibility (B) for the study population.

Statistical analysis

All data are presented as mean [range]. Data were analysed with SPSS 23.0 (SPSS, Chicago, IL, USA). Normal distribution of the data was assessed with the Shapiro-Wilk test. One way analysis of variance or Kruskal-Wallis test were used to compare extensibility, longitudinal strain, distensibility, and circumferential area change between longitudinal segments and radial intersections, respectively. Pearson's or Spearman's rank test were used to assess correlation for age and for body surface area and the observed values for extensibility and distensibility. A p -value <0.05 was considered to be statistically significant.

Differences in the 3D segmentation of the different phases of the CTA data can lead to significant differences in the definition of the lumen boundaries. Furthermore, the manual designation of the proximal and distal ends of the aortic lumen boundaries can lead to differences in the definition of centre lines and cross sectional areas. To assess this potential variability, 3D segmentations and centre lines were obtained for all cardiac phases of one patient, all measurements were calculated twice, thereby providing a measure of intra-observer variability. Bland-Altman plots were created and Lin's Concordance Correlation Coefficient (LCCC) was calculated. An LCCC of >0.99 was considered to be almost perfect agreement, 0.96 – 0.99 as substantial agreement, 0.90 – 0.95 as moderate agreement, and <0.90 as poor agreement.

Extensibility and distensibility

Circumferential and longitudinal deformations were quantified. Standard definitions^{10,11} of circumferential and longitudinal strain were used:

$$\text{circumferential area strain} = \frac{\text{maximum lumen area} - \text{minimum lumen area}}{\text{minimum lumen area}} * 100 \quad \text{unit : \%}$$

$$\text{longitudinal strain} = \frac{\text{maximum aortic length} - \text{minimum aortic length}}{\text{minimum aortic length}} * 100 \quad \text{unit : \%}$$

Additionally, the standard definition^{10,11} of distensibility was also used to characterise the circumferential deformation:

$$\text{distensibility} = \frac{\text{maximum lumen area} - \text{minimum lumen area}}{\text{minimum lumen area} * \text{pulse pressure}} \quad \text{unit : mmHg}^{-1}$$

In the longitudinal direction, a formal definition of extensibility is needed. Changes in aortic length can be understood as the result of a force pulling up and down the proximal end of the aorta. This force can be approximated to the product of blood pressure times aortic inlet cross

sectional area. Considering this, the following definition of extensibility is proposed:

$$\text{extensibility} = \frac{\text{maximum aortic length} - \text{minimum aortic length}}{\text{minimum aortic length} * \text{pulse pressure} * \text{inlet area}} \quad \text{unit : mmHg}^{-1} \text{ or } \text{N}^{-1}$$

Pulse pressure was calculated as the difference between systolic and diastolic pressure.

RESULTS

Eight patients with abdominal aortic aneurysm and two patients with thoracic aortic aneurysm were included. Mean age was 76 ± 7 years, mean pulse pressure was 67 ± 9 mmHg (see Table 1).

Aortic lengths, longitudinal strain, and extensibility

The mean length of the entire thoracic aorta varied from 293.8–444.2 mm during diastole to 299.5–457.1 during systole. Length change, extensibility, and longitudinal strain are listed in Table 2. There was substantial variation in extensibility of the entire thoracic aorta between individuals, ranging from $1.3 \times 10^{-3} \text{ N}^{-1}$ to $6.8 \times 10^{-3} \text{ N}^{-1}$, but mean extensibility was similar for patients with abdominal and thoracic aneurysms. There was significant variation between the three different segments ($p < .01$); most pronounced extensibility was observed in the ascending aorta. Mean longitudinal strain of the entire thoracic aorta amounted to 2.7%, with significant variations among the three different segments ($p < .01$); it was most pronounced in the ascending aorta and smallest in the descending aorta (see Table 2). There was no significant correlation between age and extensibility. Body surface area was significantly correlated with extensibility of the entire aorta (correlation coefficient -0.68 , $p = .03$) but not with the separate longitudinal segments.

Table 1. Study population.

ID	Sex	Age, years	Body surface area, mm ²	Aortic disease	Brachial blood pressure, mmHg
1	M	66	1.7	AAA	137/78
2	M	86	1.8	AAA	140/60
3	F	89	1.7	AAA	136/81
4	F	83	1.9	AAA	148/72
5	M	72	2.2	AAA	170/90
6	M	68	2.0	AAA	162/98
7	M	76	1.7	AAA	133/70
8	M	75	2.0	AAA	125/69
9	M	75	1.9	TAA	151/83 (84/59 after TEVAR)
10	F	77	1.8	TAA	113/45 (122/57 after TEVAR)

AAA = abdominal aortic aneurysm; TAA = thoracic aortic aneurysm.

Table 2. Aortic length change, longitudinal strain, and extensibility of entire thoracic aorta and three longitudinal segments.

	Non dilated, <i>n</i> = 8	Aneurysmal, <i>n</i> = 2	All non-stented, <i>n</i> = 10
Length change, mm			
Entire thoracic aorta	9.6 [5.6–16.0]	8.3 [3.7–12.9] <i>15.8 [7.4–24.2] after TEVAR</i>	9.4 [3.7–16.0]
Ascending aorta	7.5 [5.0–10.9]	5.1 [4.5–5.6] <i>10.5 [8.1–12.8] after TEVAR</i>	7.0 [4.5–10.9]
Aortic arch	2.1 [1.0–5.0]	2.7 [1.4–4.0] <i>8.1 [7.6–8.5] after TEVAR</i>	2.3 [1.0–5.0]
Descending aorta	5.7 [2.3–11.2]	3.6 [1.7–5.4] <i>11.0 [7.3–14.8] after TEVAR</i>	5.3 [1.7–11.2]
Extensibility, 10 ⁻³ N ⁻¹			
Entire thoracic aorta	3.9 [1.3–6.8]	1.9 [1.7–2.2] <i>5.8 [4.2–7.3] after TEVAR</i>	3.5 [1.3–6.8]
Ascending aorta	23.6 [10.2–36.2]	8.5 [5.7–11.2] <i>29.5 [14.2–44.8] after TEVAR</i>	20.6 [5.7–36.2]
Aortic arch	6.6 [24.7–22.9]	6.0 [4.4–7.6] <i>38.9 [16.7–61.1] after TEVAR</i>	6.5 [2.5–22.9]
Descending aorta	4.7 [1.9–12.3]	N/A ^a <i>10.5 [6.0–15.0] after TEVAR</i>	4.4 [1.6–12.3]
Longitudinal strain, %			
Entire thoracic aorta	2.9 [1.6–4.5]	1.9 [1.0–2.9] <i>3.8 [2.0–5.6] after TEVAR</i>	2.7 [1.0–4.5]
Ascending aorta	18.1 [12.3–31.9]	7.1 [6.6–7.7] <i>15.3 [12.1–18.6] after TEVAR</i>	15.9 [6.6–31.9]
Aortic arch	4.4 [2.0–11.2]	6.0 [3.4–8.5] <i>19.3 [16.5–22.0] after TEVAR</i>	4.7 [2.0–11.2]
Descending aorta	2.4 [1.0–4.7]	1.2 [0.7–1.7] <i>3.8 [2.8–4.7] after TEVAR</i>	2.2 [0.7–4.7]

Data presented as mean [range]. Values after TEVAR are shown in italics.

^a The luminal area at the level of the left subclavian artery could not be extracted for the pre-TEVAR CTA of one patient with thoracic aortic aneurysm, therefore the mean extensibility of the descending aorta could not be included for the two thoracic aneurysm patients.

Aortic diameters, areas, and distensibility

Mean diameters and lumen area changes, distensibility, and circumferential area strain are listed in Table 3. Systolic thoracic aortic diameter ranged from 31.2–46.2 mm at the sinotubular junction to 22.9–40.9 mm at the coeliac bifurcation. Diastolic diameter ranged from 30.3–44.1 mm at the sinotubular junction to 22.5–39.9 mm at the coeliac bifurcation. Diameter change was up to 6 mm for some patients, although in other patients, diameter changes were smaller than 0.5 mm at any level (including at the sinotubular junction). Accordingly, distensibility varied widely, ranging from $2.7 \times 10^{-3} \text{ mmHg}^{-1}$ to $25.0 \times 10^{-3} \text{ mmHg}^{-1}$ at the level of the left subclavian artery. Mean distensibility was similar for patients with abdominal and thoracic aneurysms. Mean distensibility and circumferential area strain did not differ significantly between the four studied radial intersections ($p = .236$ and $p = .211$, respectively). There was no significant correlation between age and distensibility of any of the cross sections. Body surface area showed a significant negative correlation with distensibility at the level of the brachiocephalic trunk (correlation coefficient -0.69 , $p = .026$), but not at the other cross sections.

Intra-observer repeatability

Intra-observer analysis showed a mean difference of $0.9 \pm 3.2 \text{ mm}$ ($p = .13$), with an LCCC >0.99 (95% CI >0.99

$- >0.99$) for length measurements. Mean difference was $5.8 \pm 27.8 \text{ mm}^2$ ($p = .25$) for area measurements, with an LCCC 0.98 (95% CI 0.96–0.99) and $0.1 \pm 0.5 \text{ mm}$ ($p = .21$) for maximum diameter measurements, with an LCCC of 0.99 (95% CI 0.97–0.99), as shown in Fig. 2.

DISCUSSION

The aortic deformations during the cardiac cycle, particularly those in the longitudinal direction, have been little studied. This study quantified radial expansion, or distensibility, and longitudinal expansion, or extensibility. A new definition is proposed for how the latter should be calculated, based on the physiological principle that the changes in length are caused by heart movement pulling the proximal end of the aorta up and down in combination with the load ejected into the ascending aorta. The main findings show considerable deformations in both directions for a cohort of patients with abdominal or thoracic aortic aneurysms, with important variations between individuals. Pulsatile deformations were similar for non-dilated and aneurysmal thoracic aortas. Moreover, it was found that the largest deformations occur in the ascending aorta.

The clinical importance of defining extensibility and distensibility of the thoracic aorta encompasses different areas. Firstly, it serves a purpose for pre-operative planning of aortic interventions. Typically, stent graft sizing is based on the maximum aortic diameter of the proximal landing

Table 3. Aortic diameter and area changes, distensibility, and circumferential area strain at four intersections.

	Non dilated, <i>n</i> = 8	Aneurysmal, <i>n</i> = 2	All non-stented, <i>n</i> = 10
Diameter change, mm			
Sinotubular junction	3.1 [0.5–6.7]	1.5 [0.8–2.1] <i>5.7 [3.9–7.5] after TEVAR</i>	2.7 [0.5–6.7]
Brachiocephalic trunk	1.6 [0.3–3.7]	2.4 [1.0–3.8] <i>4.4 [1.7–7.0] after TEVAR</i>	1.7 [0.3–3.8]
Left subclavian artery	1.4 [0.4–4.3]	N/A* <i>6.7 [5.1–8.2] after TEVAR</i>	1.3 [0.3–4.3]
Coeliac trunk	2.1 [0.3–4.8]	0.7 [0.4–1.0] <i>4.7 [2.9–6.4] after TEVAR</i>	1.8 [0.3–4.8]
Area change, mm²			
Sinotubular junction	97.4 [30.9–201.9]	87.3 [86.4–88.2] <i>145.5 [90.7–200.2] after TEVAR</i>	95.4 [30.9–201.9]
Brachiocephalic trunk	53.5 [23.4–118.0]	108.4 [39.4–177.3] <i>137.6 [85.8–189.4] after TEVAR</i>	64.5 [23.4–177.3]
Left subclavian artery	36.5 [10.8–81.0]	N/A* <i>73.8 [51.9–95.7] after TEVAR</i>	35.4 [10.8–81.0]
Coeliac trunk	41.5 [13.5–72.5]	26.8 [11.4–42.2] <i>82.3 [31.6–133.0] after TEVAR</i>	38.6 [11.4–72.5]
Distensibility, 10⁻³ mmHg⁻¹			
Sinotubular junction	1.7 [0.5–2.9]	1.5 [0.9–2.1] <i>3.5 [2.2–4.8] after TEVAR</i>	1.7 [0.5–2.9]
Brachiocephalic trunk	1.1 [0.3–3.3]	1.5 [0.7–2.3] <i>3.0 [2.7–3.3] after TEVAR</i>	1.2 [0.3–3.3]
Left subclavian artery	0.9 [0.3–2.5]	N/A ^a <i>2.8 [1.7–3.9] after TEVAR</i>	0.9 [0.3–2.5]
Coeliac trunk	1.3 [0.4–3.3]	0.6 [0.5–0.7] <i>2.7 [2.4–3.0] after TEVAR</i>	1.2 [0.4–3.3]
Circumferential area strain, %			
Sinotubular junction	11.6 [3.3–18.5]	10.1 [6.2–14.1] <i>13.1 [7.6–15.3] after TEVAR</i>	11.3 [3.3–18.5]
Brachiocephalic trunk	6.8 [2.2–18.4]	10.2 [4.7–15.6] <i>(13.0 ± 6.8 after TEVAR)</i>	7.5 [2.2–18.4]
Left subclavian artery	5.9 [2.2–14.0]	N/A ^a <i>(10.5 ± 1.0 after TEVAR)</i>	5.9 [2.2–14.0]
Coeliac trunk	8.7 [2.5–18.3]	3.8 [3.1–4.6] <i>(11.4 ± 5.5 after TEVAR)</i>	7.7 [2.5–18.3]

Data presented as mean [range]. Values after TEVAR are shown in italics.

^a The diameter and luminal area at the level of the left subclavian artery could not be extracted for the pre-TEVAR CTA of one patient with thoracic aortic aneurysm, therefore the mean pre-TEVAR diameter and area change, distensibility, and circumferential area strain could not be included for the two thoracic aneurysm patients.

zone. A potential measurement error of up to 5 mm should be taken into account for manual diameter measurements in the thoracic aorta.²⁰ A computer aided, semi-automatic measurement method reduces the possibilities for

customisation but may help to reduce the measurement error.²¹ The present data show similar values of ascending aortic distensibility to those found in studies using epi-aortic echography (during surgery)²² or cine-MRI

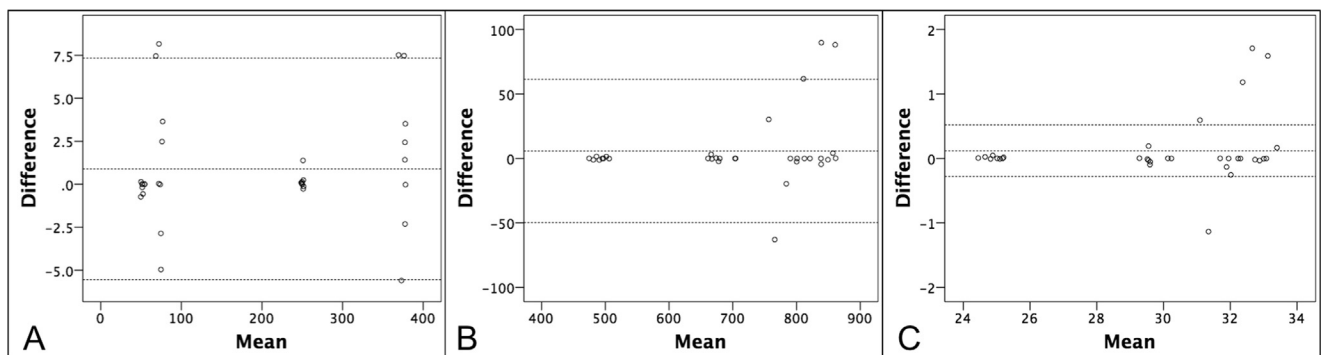


Figure 2. Bland-Altman plots showing intra-observer variability for measurements of (A) length; (B) area; (C) maximum diameter.

protocols.¹¹ Pulsatile diameter changes of up to 4.3 mm were noted in the proximal descending aorta, which is the most common landing zone. The results of semi-automatic diameter measurements show small intra-observer differences, and were thus sufficiently adequate to record diameter changes over the cardiac cycle.

Arterial stiffness is the inverse of arterial compliance. Arterial compliance is defined as the change in volume caused by a change in pressure. Distensibility is compliance divided by the initial volume, and if the artery is relatively fixed to its surroundings and the flow is pulsatile, then distensibility can be estimated as a change in cross sectional area for a change in pulse pressure.⁹ Aortic distensibility of healthy individuals decreases sharply after the age of 50,¹¹ a threshold after which most TEVAR procedures are performed. The present data show that, on average, diameter changes over the cardiac cycle are less than 2 mm in some aortic segments. However, some of the patients showed significant pulsatile diameter changes of up to 6 mm, despite advanced age. Therefore, dynamic imaging may be helpful to identify those patients with significant distensibility. ECG gated CTA has a radiation dose of about 21 mGy, which is within the range of standard abdominal CTA, but still provides images of good quality,²³ and can therefore be valuable for pre-operative evaluation prior to TEVAR to prevent incorrect stent graft sizing.

Stent graft sizing includes not only choosing the correct stent graft diameter but also the correct length. Few studies have quantified longitudinal deformations of the thoracic aorta^{10,24,25} and reference values on thoracic aortic extensibility are lacking. Descending aortic length changes ranging from 1.7 to 11.2 mm were observed, which may be a reason for choosing a slightly longer stent graft than may be initially expected, especially in the presence of important aortic tortuosity. More data on longitudinal pulsatile deformations may help to determine the correct degree of "longitudinal oversizing." Furthermore, increased longitudinal strain has been reported to be an important risk factor of aortic dissection,²⁴ which further underlines the importance of quantifying normal extensibility.

Pulsatile aortic motion has a twisting pattern. This is triggered by the load of the blood flow, pushed with force into the ascending aorta, combined with anatomical fixation by an anterior ligament at the distal arch. This twist during systole creates difficulties in measuring dimensions, especially length, in the proximal aorta, because of an out of plane movement.²⁶ At best, if there was no out of plane movement, the measured length changes of the centre lumen line would accurately represent the length changes between two anatomical landmarks. Any movement to another plane can only increase the length of the centre lumen line. Because this out of plane movement is not measured with the present method, the observed extensibility is likely to be an underestimation. Therefore, the implications of aortic extensibility for choosing the correct stent graft length are particularly important when treating aortic lesions which necessitate proximal TEVAR deployment in zone 0, as reported with increasing frequency in recent years.^{27,28}

Although the current generation of stent grafts already offers some degree of conformability to aortic pulsatile deformations, computational studies show that the stent material and graft material (i.e. nitinol and woven polyester or ePTFE), are still much stiffer than native aortic tissue.^{29,30} This may explain a native aorta to stent graft mismatch in distensibility and strain in radial and longitudinal directions.³¹ Quantification of normal pulsatile deformations can be used as a requirement for the next generations of stent grafts. Finally, assessing aortic distensibility might not only aid physicians, but also biomedical engineers. For example, this type of data can be useful for computational studies,³² which rely on clinical input data for the so called "boundary conditions" of the computational models.

A limitation of the present study is that peripheral pulse pressure rather than central aortic pressure was used to calculate aortic distensibility. The thoracic aorta is a predominantly elastic artery, while the brachial artery is a predominantly muscular artery, which leads to an impedance mismatch between the two; however, this mismatch is reduced or even reversed at advanced age.³³ Therefore, the effect of using brachial blood pressure as if it were central aortic pressure will probably be minimal for the study population. The small sample size and retrospective design are other significant limitations. Future studies involving more patients might eventually help to define more precise values of distensibility, which can be used as reference values.

In conclusion, a semi-automated measurement method based on dynamic CTA imaging of the thoracic aorta was used to quantify aortic extensibility, distensibility, and pulsatile strain. This method showed considerable deformations throughout the thoracic aorta, with notable differences between the ascending and descending aorta. As deformations were similar for non-dilated and aneurysmal thoracic aortas, the results may have implications for pre-operative planning of TEVAR for patients with aneurysm, in particular for proximal stent graft deployment. Finally, data on aortic dynamics, such as presented in this study, highlight the need for devices that can mimic the significant aortic longitudinal and circumferential strains.

CONFLICT OF INTEREST

None.

FUNDING

This work is partially funded by: ERC Starting Grant through the Project ISOBIO: Isogeometric Methods for Biomechanics (No. 259229); Ministero dell'Istruzione, dell'Università e della Ricerca through the Project no. 2010BFXRHS, iCardioCloud project by Cariplo Foundation (no. 2013–1779) and Lombardy Region (No. 42938382; No. 46554874).

REFERENCES

- 1 Dong ZH, Fu WG, Wang YQ, Guo da Q, Xu X, Ji Y, et al. Retrograde type A aortic dissection after endovascular stent graft placement for treatment of type B dissection. *Circulation* 2009;119:735–41.

- 2 Dong Z, Fu W, Wang Y, Wang C, Yan Z, Guo D, et al. Stent graft-induced new entry after endovascular repair for Stanford type B aortic dissection. *J Vasc Surg* 2010;**52**:1450–7.
- 3 Jonker FH, Schlosser FJ, Geirsson A, Sumpio BE, Moll FL, Muhs BE. Endograft collapse after thoracic endovascular aortic repair. *J Endovasc Ther* 2010;**17**:725–34.
- 4 Kasirajan K, Dake MD, Lumsden A, Bavaria J, Makaroun MS. Incidence and outcomes after infolding or collapse of thoracic stent grafts. *J Vasc Surg* 2012;**55**:652–8. discussion 8.
- 5 van Prehn J, Vincken KL, Sprinkhuizen SM, Viergever MA, van Keulen JW, van Herwaarden JA, et al. Aortic pulsatile distention in young healthy volunteers is asymmetric: analysis with ECG-gated MRI. *Eur J Vasc Endovasc Surg* 2009;**37**:168–74.
- 6 van Prehn J, Bartels LW, Mestres G, Vincken KL, Prokop M, Verhagen HJ, et al. Dynamic aortic changes in patients with thoracic aortic aneurysms evaluated with electrocardiography-triggered computed tomographic angiography before and after thoracic endovascular aneurysm repair: preliminary results. *Ann Vasc Surg* 2009;**23**:291–7.
- 7 Teutelink A, Muhs BE, Vincken KL, Bartels LW, Cornelissen SA, van Herwaarden JA, et al. Use of dynamic computed tomography to evaluate pre- and postoperative aortic changes in AAA patients undergoing endovascular aneurysm repair. *J Endovasc Ther* 2007;**14**:44–9.
- 8 Pol JA, Truijers M, van der Vliet JA, Fillinger MF, Marra SP, Renema WK, et al. Impact of dynamic computed tomographic angiography on endograft sizing for endovascular aneurysm repair. *J Endovasc Ther* 2009;**16**:546–51.
- 9 Wilmer Nichols MOR, Charalambos Vlachopoulos. *McDonald's blood flow in arteries, sixth edition. Theoretical, experimental and clinical principles.* CRC Press; 2011.
- 10 Bell V, Mitchell WA, Sigurdsson S, Westenberg JJ, Gotal JD, Torjesen AA, et al. Longitudinal and circumferential strain of the proximal aorta. *J Am Heart Assoc* 2014;**3**:e001536.
- 11 Redheuil A, Yu WC, Wu CO, Mousseaux E, de Cesare A, Yan R, et al. Reduced ascending aortic strain and distensibility: earliest manifestations of vascular aging in humans. *Hypertension* 2010;**55**:319–26.
- 12 Redheuil A, Wu CO, Kachenoura N, Ohyama Y, Yan RT, Bertoni AG, et al. Proximal aortic distensibility is an independent predictor of all-cause mortality and incident CV events: the MESA study. *J Am Coll Cardiol* 2014;**64**:2619–29.
- 13 Vlachopoulos C, Aznaouridis K, Stefanadis C. Prediction of cardiovascular events and all-cause mortality with arterial stiffness: a systematic review and meta-analysis. *J Am Coll Cardiol* 2010;**55**:1318–27.
- 14 Cavalcante JL, Lima JA, Redheuil A, Al-Mallah MH. Aortic stiffness: current understanding and future directions. *J Am Coll Cardiol* 2011;**57**:1511–22.
- 15 van Bogerijen GH, van Herwaarden JA, Conti M, Auricchio F, Rampoldi V, Trimarchi S, et al. Importance of dynamic aortic evaluation in planning TEVAR. *Ann Cardiothorac Surg* 2014;**3**:300–6.
- 16 Raaz U, Zollner AM, Schellinger IN, Toh R, Nakagami F, Brandt M, et al. Segmental aortic stiffening contributes to experimental abdominal aortic aneurysm development. *Circulation* 2015;**131**:1783–95.
- 17 Yushkevich PA, Piven J, Hazlett HC, Smith RG, Ho S, Gee JC, et al. User-guided 3D active contour segmentation of anatomical structures: significantly improved efficiency and reliability. *NeuroImage* 2006;**31**(3):1116–28.
- 18 Piccinelli M, Veneziani A, Steinman DA, Remuzzi A, Antiga L. A framework for geometric analysis of vascular structures: application to cerebral aneurysms. *IEEE Trans Med Imaging* 2009;**28**:1141–55.
- 19 Trentin C, Faggiano E, Conti M, Auricchio F. An automatic tool for thoracic aorta segmentation and 3D geometric analysis. *Image Signal Process Anal ISPA 2015 9th Int Symp* 2015:60–5.
- 20 Fillinger MF, Greenberg RK, McKinsey JF, Chaikof EL. Society for Vascular Surgery Ad Hoc Committee on TRS. Reporting standards for thoracic endovascular aortic repair (TEVAR). *J Vasc Surg* 2010;**52**:1022–1033, 33 e15.
- 21 van Keulen JW, van Herwaarden JA, Muhs BE, Verhagen HJ. Commentary: Dynamics of the aorta and the influence on stent-graft sizing. *J Endovasc Ther* 2009;**16**:552–3.
- 22 Koullias G, Modak R, Tranquilli M, Korkolis DP, Barash P, Elefteriades JA. Mechanical deterioration underlies malignant behavior of aneurysmal human ascending aorta. *J Thorac Cardiovasc Surg* 2005;**130**:677–83.
- 23 Muhs BE, Vincken KL, van Prehn J, Stone MK, Bartels LW, Prokop M, et al. Dynamic cine-CT angiography for the evaluation of the thoracic aorta: insight in dynamic changes with implications for thoracic endograft treatment. *Eur J Vasc Endovasc Surg* 2006;**32**:532–6.
- 24 Beller CJ, Labrosse MR, Thubrikar MJ, Robicsek F. Role of aortic root motion in the pathogenesis of aortic dissection. *Circulation* 2004;**109**:763–9.
- 25 Morrison TM, Choi G, Zarins CK, Taylor CA. Circumferential and longitudinal cyclic strain of the human thoracic aorta: age-related changes. *J Vasc Surg* 2009;**49**:1029–36.
- 26 Weber TF, Muller T, Biesdorf A, Worz S, Rengier F, Heye T, et al. True four-dimensional analysis of thoracic aortic displacement and distension using model-based segmentation of computed tomography angiography. *Int J Cardiovasc Imaging* 2014;**30**:185–94.
- 27 Vallabhajosyula P, Gottret J-P, Bavaria JE, Desai ND, Szeto WY. Endovascular repair of the ascending aorta in patients at high risk for open repair. *J Thorac Cardiovasc Surg* 2015;**149**:S144–50.
- 28 Piffaretti G, Galli M, Lomazzi C, Franchin M, Castelli P, Mariscalco G, et al. Endograft repair for pseudoaneurysms and penetrating ulcers of the ascending aorta. *J Thorac Cardiovasc Surg* 2016;**151**:1606–14.
- 29 Roccabianca S, Figueroa CA, Tellides G, Humphrey JD. Quantification of regional differences in aortic stiffness in the aging human. *J Mech Behav Biomed Mater* 2014;**29**:618–34.
- 30 Kleinstreuer C, Li Z, Basciano CA, Seelecke S, Farber MA. Computational mechanics of Nitinol stent grafts. *J Biomech* 2008;**41**:2370–8.
- 31 Nauta FJ, Conti M, Kamman AV, van Bogerijen GH, Tolenaar JL, Auricchio F, et al. Biomechanical changes after thoracic endovascular aortic repair in type B dissection: a systematic review. *J Endovasc Ther* 2015;**22**:918–33.
- 32 van Bogerijen GH, Auricchio F, Conti M, Lefieux A, Reali A, Veneziani A, et al. Aortic hemodynamics after thoracic endovascular aortic repair, with particular attention to the bird-beak configuration. *J Endovasc Ther* 2014;**21**:791–802.
- 33 Mitchell GF, Parise H, Benjamin EJ, Larson MG, Keyes MJ, Vita JA, et al. Changes in arterial stiffness and wave reflection with advancing age in healthy men and women: the Framingham Heart Study. *Hypertension* 2004;**43**:1239–45.